Transceiver Impairment Mitigation by 8×2 Widely Linear MIMO Equalizer With Independent Complex Filtering on IQ Signals

Masaki Sato, Manabu Arikawa, Hidemi Noguchi, Junichiro Matsui, Jun'ichi Abe, and Emmanuel Le Taillandier de Gabory

***Abstract*—High-order modulation formats with high symbol rates are promising candidates for meeting the growing traffic requirements of digital coherent transmission. In using these modulation formats, the impact of transceiver impairment on the signal quality becomes significant. In this paper, we propose an 8×2 widely linear (WL) multiple-input multiple-output (MIMO) equalizer with independent complex filtering on IQ signals to mitigate linear transceiver impairments. Furthermore, we extend the equalizer for digital subcarrier (SC) multiplexing. Accordingly, a 16×4 WL MIMO equalizer is also proposed to mitigate linear transceiver impairments, through application to a pair of SC inputs. Experimental results show that, for transmission of a 58-GBaud polarization-multiplexing 64 quadrature amplitude modulation (PM-64QAM) single-carrier signal, the proposed method effectively compensates for various receiver impairments and also mitigates transmitter (Tx) impairments. Q-penalties of 0.1 dB up to a 10-ps skew, 2.5-dB gain imbalance, 7.2-degree phase error, and –15-dB crosstalk in Tx were achieved for 100-km standard single-mode fiber transmission. Moreover, for a 29-GBaud PM-64QAM dual-SC signal, the proposed 16 × 4 WL MIMO equalizer shows transceiver impairment mitigation performance similar to that in the single-carrier case, even though dual-SC transmission is less tolerant of laser phase noise.**

***Index Terms*—Digital coherent transmission, digital signal processing, multiple-input multiple-output, optical fiber communication, quadrature amplitude modulation.**

I. Introduction

DIGITAL coherent transmission is a key to handling the accelerating growth in global traffic demand. In this regard, a higher symbol rate and higher-order modulation are desirable [1]. As the symbol rate increases, the signal-quality impact of linear impairments such as various IQ imbalances, either frequency dependent or independent, becomes more significant in proportion to the modulation order. Accordingly, several transceiver impairment mitigation techniques featuring digital signal processing (DSP) have been proposed, for both factory calibration [2] and adaptive equalization at the coherent receiver [3]–[11].

Digital subcarrier (SC) multiplexing, in which a single carrier is split into digital SCs, is also gaining attention, because it has several benefits for both linear and nonlinear tolerance [10]–[12]. It is also suitable for systems with high symbol rates, as flexible data allocation for SCs may enhance the spectral efficiency because of the limited device bandwidth. However, there are some drawbacks to the digital SC approach: in comparison to the single-carrier approach, it is more sensitive to transceiver impairments [11], and it is less tolerant of laser phase noise, because the symbol rate of an SC is equal to the symbol rate of a single carrier divided by the number of SCs [14]. Hence, transceiver impairment mitigation techniques are mandatory for digital SC multiplexing systems.

Transceiver impairments are often separately discussed for a transmitter (Tx) and a receiver (Rx). To mitigate Tx impairment, a 2×2 real-IQ multiple-input multiple-output (MIMO) equalizer for signals after carrier phase recovery (CPR) has been proposed [4]. We have also proposed a 4×2 widely linear (WL) MIMO equalizer embedding preliminary CPR [5]. This equalizer first compensates for carrier phase error and then compensates simultaneously for polarization rotation and Tx impairments. Through joint calculation of the filter coefficients and carrier phase by using the MIMO equalizer's output, IQ imbalance mitigation without contamination from excessive impairment has been demonstrated [4]. As for mitigation of Rx impairment, a complex 4×2 MIMO equalizer with independent chromatic dispersion compensation (CDC) has been proposed [3]. In another approach, the complex 4×2 MIMO equalizer with independent CDC was concatenated with the Gram-Schmidt orthogonalization procedure for Rx impairment mitigation, and Tx impairment was separately compensated by a 4×4 real-IQ MIMO equalizer after CPR [6].

To improve the signal quality of the high-order modulation format, a joint equalization scheme for both Tx and Rx impairment is desirable, as this format is vulnerable to IQ imbalance. A multi-layer filter architecture that is based on a physical model and adaptively updates all the coefficients via back-propagation from the last outputs has been proposed

Manuscript received March 10, 2022; revised April 22, 2022; accepted May 4, 2022. Date of publication May 10, 2022; date of current version May 26, 2022. This work was supported in part by the Research and Development of Innovative Optical Network Technology as a new Social Infrastructure of the Ministry of Internal Affairs and Communications Japan under Grant JPMI00316. *(Corresponding author: Masaki Sato.)*

Masaki Sato, Manabu Arikawa, Hidemi Noguchi, Jun'ichi Abe, and Emmanuel Le Taillandier de Gabory are with the System Platform Research Laboratories, NEC Corporation, Kawasaki 211-8666, Japan (e-mail: m-satou-kj@nec.com; marikawa@nec.com; h-noguchi_da@nec.com; abe.junichi@nec.com; eltdg@nec.com).

Junichiro Matsui is with the 1st Network Solutions Division, NEC Corporation, Chiba 270-1198, Japan (e-mail: junichiro.matsui@nec.com).

Digital Object Identifier 10.1109/JPHOT.2022.3173652

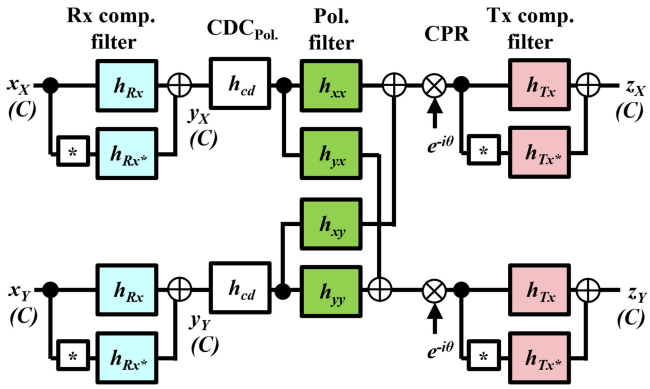

Fig. 1. Ideal signal demodulation process (C: complex).

[7]. This architecture demonstrated IQ skew compensation for both Tx and Rx. However, the relatively long feedback loop in the circuit implementation for the multi-layer filter might be a disadvantage. Consolidation of filters would be one option to keep the circuit resources within a reasonable scale.

To tackle this problem, a complex 8×2 MIMO equalizer with independent CDC was proposed to simultaneously compensate for polarization rotation, Tx impairments, and Rx impairments by means of a single equalizer [8]. As with the complex 4×2 MIMO equalizer [3], the combination of independent CDC and a complex MIMO equalizer enables Rx impairment mitigation, while embedded carrier frequency offset (FO) compensation enables Tx impairment mitigation. In a similar vein, a joint FO and Tx/Rx IQ imbalance compensation scheme has been proposed for wireless MIMO orthogonal frequency-division multiplexing (OFDM) systems [9]. To compensate for transceiver impairments, however, the equalizer must take the carrier phase error into account, not just the FO.

In this paper, we propose an 8×2 WL MIMO equalizer with independent complex filtering on IQ signals. Our method compensates for polarization rotation, Tx impairments, Rx impairments, and carrier phase error with the FO by means of a single equalizer. We analytically show that the proposed method is equivalent to the ideal signal demodulation process [7]. The filter coefficients and carrier phase are jointly calculated by using the equalizer's output.

Furthermore, we extend the equalizer configuration for digital SC multiplexing: specifically, a 16×4 WL MIMO equalizer is proposed for application to a pair of SCs to mitigate transceiver impairments. We experimentally demonstrate the proposed method for both 58-Gbaud PM-64QAM and 29-Gbaud dual-SC PM-64QAM transmission. The results show that it can effectively mitigate various Tx impairments and compensate various Rx impairments in 100-km standard single-mode fiber (SSMF) transmission.

II. WL MIMO Equalizer With Independent Complex Filtering on IQ Signals

The ideal signal demodulation process with multiple filters, which is based on a physical model [7], is depicted in Fig. 1. First, the input complex-valued signals x_X and x_Y for both X and Y polarization are fed into each 2×1 WL MIMO equalizer to compensate individually for Rx impairments. Note that a 2×1 WL MIMO equalizer is equivalent to a 2×2 real-IQ MIMO equalizer [7].

Next, CDC is applied to each polarization signal, and a 2×2 strictly linear (SL) MIMO equalizer is implemented to adaptively compensate for polarization mode dispersion (PMD) and demultiplexing polarization. Note that we refer to a conventional complex-valued filter as SL in this work [7]. CPR compensates for the carrier phase error with FO compensation for each polarization. Finally, Tx impairments are compensated by a 2×1 WL MIMO equalizer for each polarization.

This model can be expressed by the equations below. For simplicity, only one polarization is described here, and the polarization filter is thus omitted. The single-polarization model is sufficient for our work, as two orthogonal polarizations are commonly handled independently. The number of taps for filters is also omitted for the same reason, and accordingly, multiplication is used instead of the convolution operation to describe the filtering process in the time domain. Same analysis also holds in the case with multiple taps since laser phase noise is slow evolving phenomena, compared with the sampling rate. The output samples z are described as follows:

$$y = h_{cd}\ \left(h_{Rx}x + h_{Rx*}x^*\right), \tag{1}$$

$$\begin{aligned} z &= h_{Tx}\ \mathrm{y}e^{-i\theta} + h_{Tx*}\left(\mathrm{y}e^{-i\theta}\right)^* \\ &= h_{Tx}\ h_{Rx}h_{cd}xe^{-i\theta} + h_{Tx}h_{Rx*}h_{cd}x^*e^{-i\theta} \\ &\quad + h_{Tx*}(h_{Rx*})^*h_{cd}^*xe^{i\theta} + h_{Tx*}h_{Rx}^*h_{cd}^*x^*e^{i\theta}. \end{aligned} \tag{2}$$

Here, x is the input samples, y is the output samples of the Rx compensation filter, θ is the compensated phases, and h_{Rx}, h_{cd}, and h_{Tx} are the filter coefficients for the Rx compensation filter, CDC, and the Tx compensation filter, respectively. Note that we treat θ as constant in (2), because phase noise is a slowly varying phenomenon in comparison with the symbol rate, and we thus assume that the impact of phase variation is small.

The proposed 8×2 WL MIMO equalizer with independent complex filtering on IQ signals is shown in Fig. 2. In contrast to the ideal signal demodulation process described above, CDC is independently applied to real signals x_{XI}, x_{XQ}, x_{YI}, and x_{YQ}, and the output signals are converted to complex signals y_{XI}, y_{XQ}, y_{YI}, and y_{YQ} [3], [8]. These signals and their conjugate signals are fed into a least mean square (LMS) -based 8×2 WL MIMO equalizer. The recovered phase, including the FO, is applied to the intermediate signals s_X and s_Y, and the conjugate of the phase is then applied to s_{X*} and s_{Y*}. Finally, the output signals z_X and $z_{Y,}$ are obtained by combining s_X, s_{X*} and s_Y, s_{Y*}, respectively. In this work, a data-aided phase-locked loop (PLL) using pilot symbols is applied for carrier recovery and is embedded in the LMS equalizer to update the filter tap coefficients by using z_X and $z_{Y,}$.

The equations below characterize the proposed method. Again, a single polarization is used, and the number of taps for filters is omitted for simplicity. Accordingly, these equations

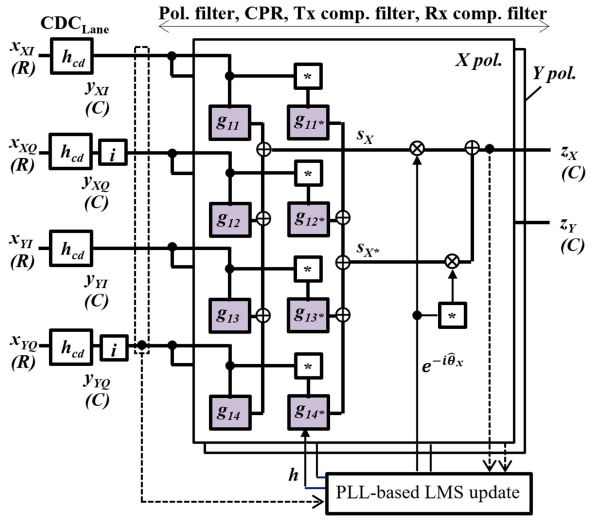

Fig. 2. Proposed 8×2 WL MIMO equalizer (R: real; C: complex; *: conjugate; pol.: polarization).

describe a 4×1 WL MIMO equalizer configuration. Also, multiplication is again used instead of the convolution operation to describe the filtering process in the time domain. The output samples z are then described as follows:

$$y_I = h_{cd}\, x_I, \;\; y_Q = h_{cd}\, x_Q, \tag{3}$$

$$\begin{aligned} z &= g_{11}\, y_I e^{-i\hat{\theta}} + g_{13}\,(iy_Q)\, e^{-i\hat{\theta}} + g_{12} y_I^* e^{i\hat{\theta}} + g_{14}(iy_Q)^* e^{i\hat{\theta}} \\ &= \left(g_{11} h_{cd} \frac{x + x^*}{2} + i g_{13} h_{cd} \frac{x - x^*}{2i} \right) e^{-i\hat{\theta}} \\ &\quad + \left(g_{12} h_{cd}^* \frac{x + x^*}{2} - i g_{14} h_{cd}^* \frac{x - x^*}{2i} \right) e^{i\hat{\theta}} \\ &= \frac{g_{11} + g_{13}}{2}\, h_{cd} x e^{-i\hat{\theta}} + \frac{g_{11} - g_{13}}{2} h_{cd} x^* e^{-i\hat{\theta}} \\ &\quad + \frac{g_{12} - g_{14}}{2} h_{cd}^* x e^{i\hat{\theta}} + \frac{g_{12} + g_{14}}{2} h_{cd}^* x^* e^{i\hat{\theta}}. \end{aligned} \tag{4}$$

Here, $x = x_I + i x_q$ is the input samples, x_I and x_Q are the respective real-valued I and Q components, $\hat{\theta}$ is the compensated phases, and g and h_{cd} are the filter coefficients for the 4 × 1 WL MIMO equalizer and independent CDC, respectively. As in (2), we treat $\hat{\theta}$ as constant.

By comparing each term of the right sides of Eqs. (2) and (4), the comparative relationship is obtained as

$$\begin{aligned} \begin{pmatrix} h_{Tx} h_{Rx} \\ h_{Tx} h_{Rx*} \end{pmatrix} &= \frac{1}{2} \begin{pmatrix} 1 & 1 \\ 1 & -1 \end{pmatrix} \begin{pmatrix} g_{11} \\ g_{13} \end{pmatrix}, \\ \begin{pmatrix} h_{Tx*} h_{Rx*}^* \\ h_{Tx*} h_{Rx}^* \end{pmatrix} &= \frac{1}{2} \begin{pmatrix} 1 & -1 \\ 1 & 1 \end{pmatrix} \begin{pmatrix} g_{12} \\ g_{14} \end{pmatrix}. \end{aligned} \tag{5}$$

On the basis of this equation, the proposed WL MIMO equalizer is equivalent to the ideal signal demodulation process with multiple filters, which means that Tx and Rx impairment compensation is enabled by the aggregated equalizer configuration. The complex 8×2 MIMO equalizer [8] is not sufficient to compensate for transceiver impairments because $\hat{\theta}$ includes only the FO, lack of the phase offset compensation may degrade the performance, whereas the proposed method includes both the FO and the phase offset for $\hat{\theta}$ in the above equations.

For reference, Rx impairment compensation is also enabled by 4×2 WL MIMO equalizer under the back-to-back condition. In ref [7], 4×2 WL MIMO equalizer was analyzed in detail for Tx skew and Rx skew with and without transmission. In situations where CD exists in the transmission line, 4×2 WL MIMO equalizer cannot compensate for Rx impairment, so complex 4×2 MIMO equalizer with independent CDC [3] is required to compensate for Rx impairment. However, both equalizers cannot compensate for Tx impairment since Tx impairment compensation is essentially needed to be carried out after CPR as described in Fig. 1.

The next issue is that, as shown in Fig. 1, CPR is individually performed prior to the Tx compensation filters. This induces CPR contamination and thus results in performance degradation with excessive Tx impairments. Even though the Tx compensation filters mitigate the degradation, CPR is compromised and enhances the phase error.

To solve this issue, one option is to use a multi-layer filter architecture [7], as it adaptively updates all the coefficients with back-propagation from the last outputs. Ref. [4] notes that a second stage of CPR after the Tx compensation filter is expected to prevent the degradation. In addition, the placement of CPR after the MIMO equalizer in the proposed method can prevent it [5].

The output samples z of the proposed 8×2 WL MIMO equalizer are described as follows:

$$\begin{aligned} z_i[k] &= \left(\sum_{j,m} g_{ij}[m]\, y_j[k-m] \right) e^{-i\hat{\theta}_i[k]} \\ &\quad + \left(\sum_{j,m} g_{ij*}[m]\, y_j^*[k-m] \right) e^{i\hat{\theta}_i[k]}. \end{aligned} \tag{6}$$

Here, y is the input samples after CDC, θ is the compensated phases, j is the input vector's index, i is the output vector's index, m is the number of taps, and k is the sample time. The filter tap coefficients g_{ij} and g_{ij*} are updated as follows:

$$\begin{aligned} g_{ij}[m] &\rightarrow g_{ij}[m] + 2\alpha l[k]_i e^{i\hat{\theta}_i[k]} y_j^*[k-m], \\ g_{ij*}[m] &\rightarrow g_{ij*}[m] + 2\alpha l[k]_i e^{-i\hat{\theta}_i[k]} y_j[k-m]. \end{aligned} \tag{7}$$

Here, μ is the step size, and l is the error between the pilot symbols p and the output samples z, where

$$l_i[k] = p_i[k] - z_i[k]. \tag{8}$$

Fig. 3 shows a block diagram of the data-aided PLL [13], [14] used in this work. The input symbol s_k is compared with the pilot symbol p_k to get the phase error e_k. We use this approach in combination with a decision-directed method to get e_k. Then, the phase error is multiplied by a weighting parameter w and fed into a loop filter for phase tracking. The phase offset θ_{f} from the FO is added to the output phase θ_{pk}. Finally, $\hat{\theta}_{\mathrm{k}}$ is applied to recover the phase of the input symbol s_k, thus generating the output symbol z_k. As described above, the first-order PLL is

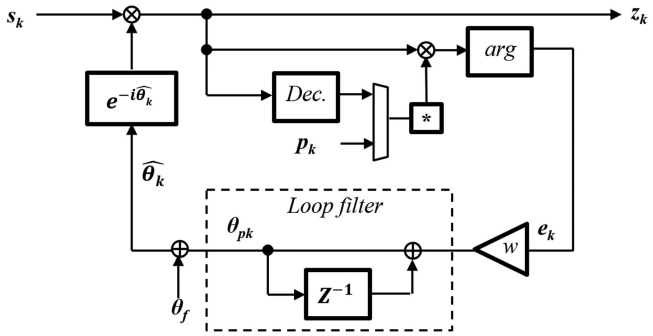

Fig. 3. Data-aided PLL for carrier recovery.

used to track the carrier phase, so our data-aided PLL requires the FO information in advance. Note that the feedback delay and parallelization delay for the implementation are not covered in this paper, but their details are described in ref. [13].

Next, the proposed WL MIMO equalizer is modified for digital SC multiplexing. For a PM digital SC signal, the WL MIMO equalizer is applied to each pair of an SC and the conjugate SC [9]–[11]. Accordingly, a 16×4 WL MIMO equalizer is used for the two SC signals with both polarizations; *e.g.*, four SCs use two sets of 16×4 WL MIMO equalizers. Fig. 4 illustrates the proposed 16×4 WL MIMO equalizer with independent complex filtering on IQ signals for digital SC signals.

First, CDC is independently applied to the input real signals x_{XI}, x_{XQ}, x_{YI}, and x_{YQ}, and the output signals are converted to complex signals y_{XI}, y_{XQ}, y_{YI}, and y_{YQ}, as in the single-carrier case with the 8×2 WL MIMO equalizer. A pair of SCs is thus demultiplexed from the digital SC signal [10]. The complex signals y_{1XI}, y_{1XQ}, y_{1YI}, y_{1YQ}, y_{2XI}, y_{2XQ}, y_{2YI}, and y_{2YQ} and their conjugate signals are fed to an LMS-based 16×4 WL MIMO equalizer. Next, the recovered phase, including the FO, is applied to the intermediate signals s_{1X}, s_{1Y}, s_{2X}, and s_{2Y}, and the conjugate of the phase is applied to each of s_{1X*}, s_{1Y*}, s_{2X*}, and s_{2Y*}. Finally, the output signals z_{1X}, z_{1Y}, z_{2X}, and z_{2Y} are obtained by combining s_{1X} and s_{1X*}, $s_{1Y,}$ and s_{2Y*}, s_{2X} and s_{2X*}, and s_{2Y} and s_{2Y*}, respectively. As in the single-carrier case, a data-aided PLL is applied for carrier recovery and is embedded in the LMS equalizer to update the filter tap coefficients by using z_{1X}, z_{1Y}, z_{2X}, and z_{2Y}.

III. Experimental Setup

We experimentally evaluated the effectiveness of the proposed method by testing 58-GBaud root-raised-cosine (RRC) -filtering PM-64QAM transmission. A roll-off factor of 0.05 was used. Transceiver impairments were digitally emulated in both Tx and Rx, as it was difficult to set up the experiment for a precise, wide range of these impairments. IQ skew, IQ imbalance, phase error, and IQ crosstalk were used to examine typical transceiver impairments. We also evaluated the effectiveness of the proposed method by testing 29-GBaud dual-SC PM-64QAM transmission, because the penalty from laser phase noise becomes more severe as the symbol rate decreases [14], [15]. On the other hand, an SC signal shows a relatively low impact from equalization-enhanced phase noise (EEPN) after transmission, but EEPN is outside the scope of this paper; instead, the details are described in ref. [15]. The 29-GBaud signals were separated by 1.8-GHz guard bands.

Fig. 5(a) shows the experimental setup. External cavity lasers (ECLs) with a mass-produced 100-kHz linewidth were used for both the signal source and the local oscillator (LO), and they were set to 1550.1 nm. The FO between the signal source and LO was set to around 1.1 GHz. On the Tx side, the electrical signal was modulated with a PM-IQ modulator and four 120-GSa/s digital-to-analog converters (DACs) after compensation of the frontend imperfections. Forward error correction (FEC) of low-density parity-check code for DVBS-2 was used with a frame length of 64,800 and a code rate of 4/5. Eight FEC frames were generated for each polarization by loading random bits to their payload; then, they were mapped to PM-64QAM through gray mapping. In this experiment, a pilot sequence was inserted for each polarization to perform pilot-based DSP [16]. One pilot symbol of quadrature phase-shift keying (QPSK) was inserted every 25 symbols, and an overhead of 2^{10} QPSK symbols was also inserted for pre-convergence of the MIMO equalizer. Tx impairments were digitally emulated for the X polarization signal, except for the quadrature phase (i.e., the phase error), which was manually shifted for X polarization. For the transmission line, we used 100 km of SSMF after polarization scrambling at a rate of 100 rad/s with an erbium-doped fiber amplifier (EDFA) amplification. The fiber launch power was set to –2 dBm to reduce the penalties due to fiber nonlinearity, which resulted in a received optical signal-to-noise ratio (OSNR) of 30.8 dB/0.1 nm. The optical signal was captured by the coherent receiver while passing through an optical bandpass filter (OBPF), after which it was converted to the electrical domain by four 256-GSa/s analog-to-digital-converters (ADCs). Finally, Rx impairments were digitally emulated for the X polarization signal of the ADC outputs. Rx X phase error is described as follows:

$$x_I + e^{\left[i\left(\frac{\pi}{2}+p_{err}\right)\right]}x_Q. \tag{9}$$

Here, x_I and x_Q are the X polarization signal of the ADC outputs, p_{err} is the phase error.

Fig. 5(b) shows the IQ crosstalk model used in this work. The crosstalk was calculated from the magnitude response to emulate the capacitive and inductive coupling characteristics between adjacent signal traces on the printed circuit board, as defined by the crosstalk level at half the symbol rate (i.e., 29 GHz). Fig. 5(c) shows the optical spectra of the 58-GBaud and 29-GBaud dual-SC PM-64QAM signals before the OBPF with a 0.02-nm resolution.

Fig. 6(a) shows the offline single-carrier DSP used in this study. The received signal was first resampled to 2 Sa/sym. Then, a fixed Rx frontend compensation filter was applied, and CDC and the matched RRC filter to prevent inter-symbol interference due to the sharp roll-off factor were applied in the frequency domain for each lane. Frame synchronization was performed

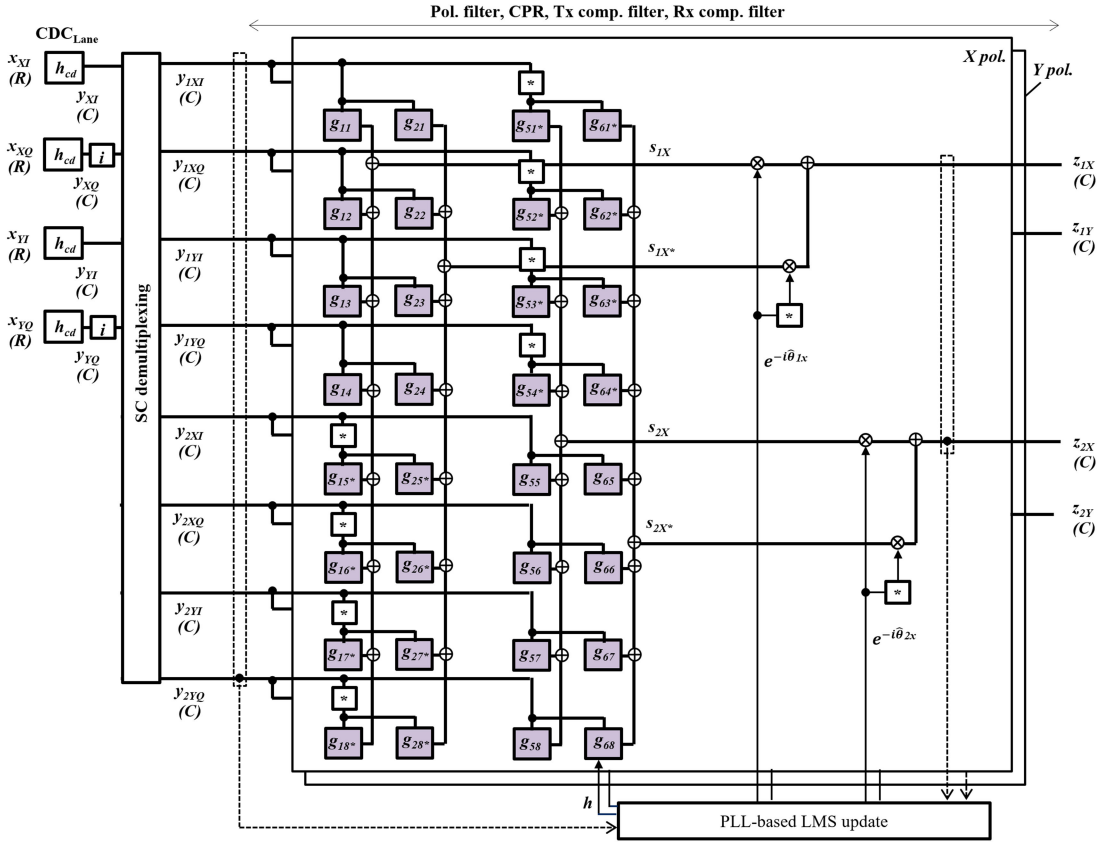

Fig. 4. Proposed 16×4 WL MIMO equalizer for digital SC signals (R: real; C: complex; *: conjugate; pol.: polarization).

by correlation to the known overhead [16] after blind polarization demultiplexing by the constant modulus algorithm and FO compensation. The polarization demultiplexing used a seven-tap 2×2 SL MIMO equalizer, and the FO compensation was based on the fourth power of the received signal. Once the location of the overhead was detected, three different MIMO equalizer configurations were evaluated: (1) a 2×2 SL MIMO equalizer, (2) a complex 8×2 MIMO equalizer [8], and (3) the proposed 8×2 WL MIMO equalizer. For all configurations, as described in the previous section, a data-aided PLL using QPSK pilot symbols was applied for carrier recovery and was embedded in the LMS equalizer to update the filter tap coefficients. The tap length of the filter was set to 21, and the QPSK overhead was used for pre-convergence of the MIMO equalizer, as described above. For the complex 8×2 MIMO equalizer, the FO value obtained from overhead detection and its conjugate were applied to each intermediate signal s_X, s_Y and s_{X*}, s_{Y*}, and the carrier phase was compensated for the output signals z_X and $z_{Y,}$. For the 8×2 WL configuration, the FO value was also fed to the PLL-based phase recovery. Once the signals were demodulated, the pilot and the overhead were removed, and the Q-factor (i.e., the pre-FEC bit error rate, or BER) was calculated. The post-FEC BER was calculated after FEC decoding.

Fig. 6(b) shows the offline DSP for the dual-SC signal. The signal processing was jointly applied to the dual SCs up to CDC. Next, subcarrier demultiplexing [10] with subsequent matched RRC filtering was applied to separate the SCs, and three different MIMO equalizer configurations were evaluated: (1) a 2×2 SL MIMO equalizer for each SC, (2) a complex 16×4 MIMO equalizer, and (3) the proposed 16×4 WL MIMO equalizer. Note that case (1) did not include any inter-SC MIMO processing, which resulted in less IQ impairment tolerance than with a single carrier [11]. The remaining processing was the same as in the single-carrier case but was applied to each SC.

IV. Results and Discussion

We first evaluated the Tx impairment mitigation performance of the 8×2 WL MIMO equalizer for 58-GBaud PM-64QAM transmission, with the complex 8×2 MIMO equalizer's performance as a baseline. In addition, the 2×2 SL MIMO equalizer was used to measure the impact of Tx impairments. Overall, even without additional impairments, the transceiver mitigation techniques compensated for residual impairments, which mainly derived from the frequency response deviations of the frontend devices. Specifically, the Q-factor was improved by 0.15 dB for both the complex 8×2 MIMO equalizer and the 8×2 WL equalizer. This result demonstrated the need for adaptive impairment mitigation. Even though precise fixed transceiver impairment mitigation was realized with excellent performance, notably enabling the transmission of 48-GBaud PM-256QAM signal 100-km [2], adaptive equalization is required to maintain the signal quality of high order QAM signals during operation of the system as impairments are not fixed. With the 8×2 WL

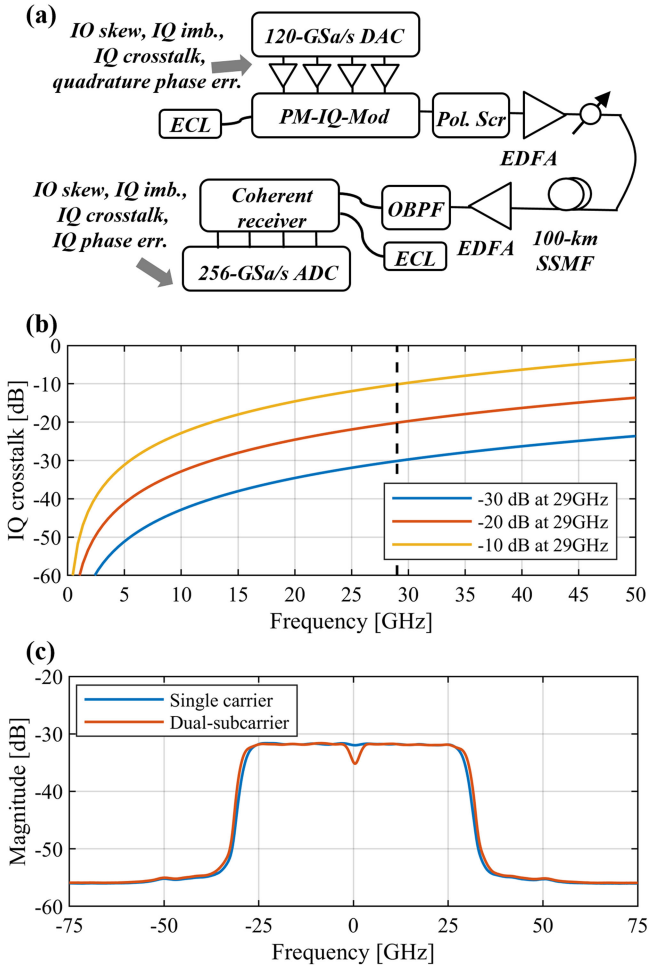

Fig. 5. Experimental setup, including (a) the setup with transceiver impairment emulation, (b) the IQ crosstalk model, and (c) the optical signal spectra.

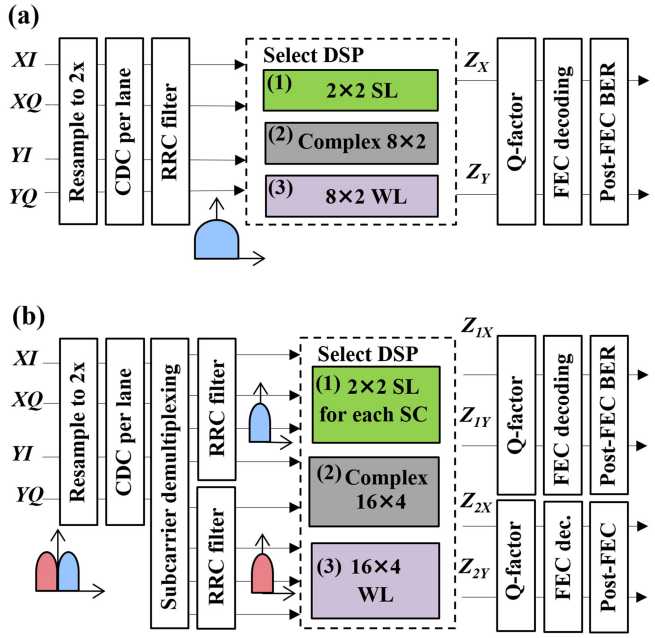

Fig. 6. Offline DSP for the (a) Single-carrier and (b) Dual-SC setups.

equalizer, Q-factor was 6.8-dB. Q-penalty at 30.8 dB/0.1 nm was 4.5-dB, compared with theoretical value.

In Fig. 7(a), the Q-factor is plotted as a function of the X-IQ skew. Note that the Q-factor was averaged over two polarization signals. We can clearly see that the 8×2 WL MIMO equalizer outperformed the others. The 2×2 SL MIMO equalizer suffered from IQ skew imbalance, which linearly degraded the Q-factor. The complex 8×2 MIMO equalizer mitigated the IQ skew somewhat, but the Q-penalty gradually increased as the skew increased because of the lack of phase compensation, as described above. As for the proposed method, a Q-penalty of 0.1 dB appeared only at 10 ps, i.e., at 0.6 unit interval (UI), which is far larger than the specifications of available frontend components; in contrast, the complex 8×2 MIMO equalizer resulted in a Q-penalty greater than 5 dB. The insets in Fig. 7(a) show constellations of the X polarization at 5 ps. The proposed 8×2 WL MIMO equalizer mitigated the Tx skew to recover a clear constellation, whereas the other two constellations were distorted.

In Fig. 7(b), the Q-factor is plotted as a function of the X-IQ gain imbalance. The 2×2 SL MIMO equalizer exhibited linear degradation as the IQ gain imbalance increased. In contrast, the 8×2 WL MIMO equalizer compensated for most of the gain imbalance. However, the Q-factor gradually decreased as the gain imbalance increased, which led to a polarization-dependent loss. Nevertheless, for a 2.5-dB gain imbalance, the proposed method exhibited a 0.1-dB Q-penalty, whereas the complex 8×2 MIMO equalizer had a 0.7-dB Q-penalty.

Next, Fig. 7(c) plots the Q-factor as a function of the quadrature phase error of the X polarization. The phase error gradually degraded the 2×2 SL MIMO equalizer's performance, whereas for the 8×2 WL MIMO equalizer, only 0.1-dB Q-penalties were observed up to 7.2 degrees, and a Q-penalty of 0.4 dB appeared at 10 degrees. The complex 8×2 MIMO equalizer also compensated successfully up to a 7.2-degree phase error, with 0.3-dB Q-penalties, but excessive error degraded the performance: a 10-degree phase error resulted in a 1.7-dB Q-penalty.

Lastly, the IQ crosstalk tolerance was evaluated. Fig. 7(d) plots the Q-factor as a function of the X-IQ crosstalk. Similarly to the previous cases, the Q-penalties for the 2×2 SL MIMO equalizer increased with the crosstalk. In contrast, the 8×2 WL MIMO equalizer outperformed the others: only 0.1-dB Q-penalties were observed up to a crosstalk of –15 dB, and a Q-penalty of 0.3 dB appeared at 10 degrees. The complex 8×2 MIMO equalizer also compensated successfully up to –15 dB, with 0.1-dB Q-penalties, but 10-dB crosstalk resulted in a 1.8-dB Q-penalty.

In the second part of the experiment, we evaluated the Rx impairment mitigation performance for 58-GBaud PM-64QAM transmission. In Fig. 8(a)–(d), the Q-factor is plotted as a function of the X-IQ skew, X-IQ imbalance, X phase error, and X-IQ crosstalk, respectively. For all cases, the 2×2 SL MIMO equalizer's performance deteriorated as the impairment increased. With the 8×2 WL MIMO equalizer, however, no Q-penalties were observed up to a 10-ps skew, 5-dB gain

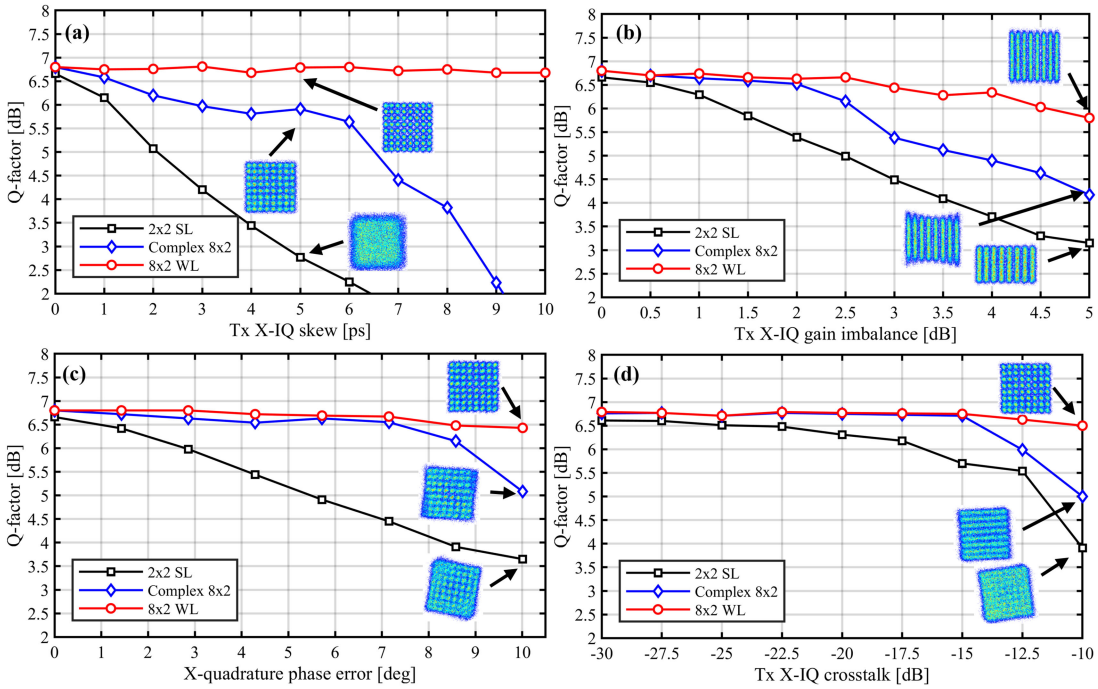

Fig. 7. Experimental results for 58-GBaud PM-64QAM transmission with Tx impairments: (a) X-IQ skew, (b) X-IQ gain imbalance, (c) X-quadrature phase error, and (d) X-IQ crosstalk.

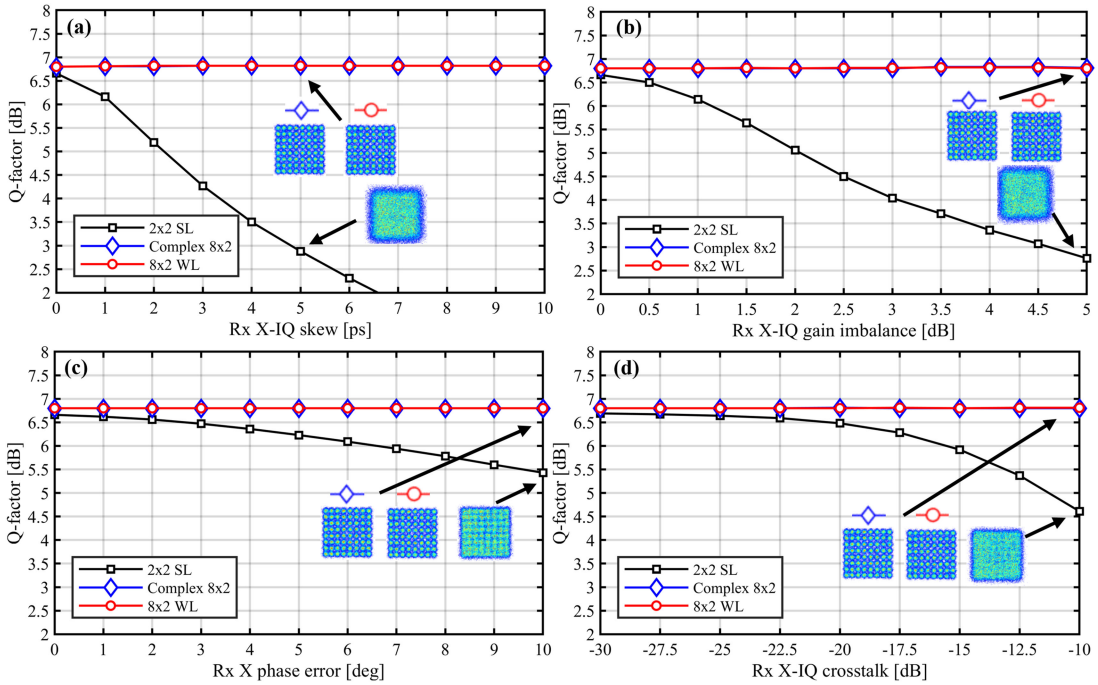

Fig. 8. Experimental results for 58-GBaud PM-64QAM transmission with Rx impairments: (a) X-IQ skew, (b) X-IQ gain imbalance, (c) X phase error, and (d) X-IQ crosstalk.

imbalance, 10-degree phase error, and –10-dB crosstalk. Excess Rx impairments might induce some penalty due to frame synchronization error, but the above values are sufficient for practical evaluation. Interestingly, the complex 8×2 MIMO equalizer also showed no Q-penalties when the Rx impairments increased. We assume the reason was that when Rx compensation proceeds smoothly before CPR, it is unaffected by insufficient phase recovery. As a result, the proposed method is beneficial for Tx impairment mitigation, as compared with the conventional complex 8×2 MIMO equalizer.

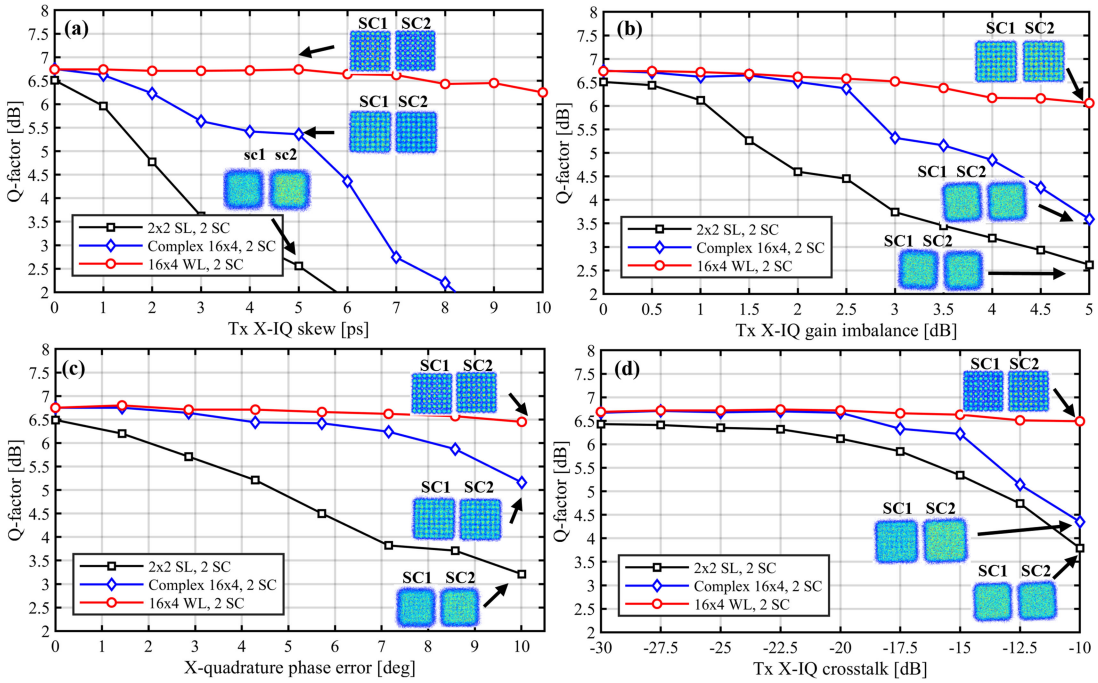

Fig. 9. Experimental results for 29-GBaud dual-SC PM-64QAM transmission with Tx impairments: (a) X-IQ skew, (b) X-IQ gain imbalance, (c) X-quadrature phase error, and (d) X-IQ crosstalk.

Next, we evaluated the Tx impairment mitigation performance of the 16×4 WL MIMO equalizer for 29-GBaud dual-SC PM-64QAM transmission, with the complex 16×4 MIMO equalizer's performance as a baseline. In addition, the application of a 2×2 SL MIMO equalizer for each SC was used to measure the impact of Tx impairments. Without additional impairments, the Q-factor was similar to that in the single-carrier case: 6.5 dB with the 2×2 SL MIMO equalizer, which was 0.15 dB lower than for a single carrier. Under the same conditions, the transceiver mitigation techniques compensated for residual impairments of the dual-SC signal, as they improved the Q-factor by 0.25 dB for both the complex 16×4 MIMO equalizer and the 16×4 WL MIMO equalizer.

In Fig. 9(a)–(d), the Q-factor is plotted as a function of the X-IQ skew, X-IQ imbalance, X-phase error, and X-IQ crosstalk, respectively. Note that the Q-factor was averaged over two polarization signals for dual-SC transmission. For all cases, the 2×2 SL MIMO equalizer's performance deteriorated as the impairment increased. The overall trends in the Q-penalty were somewhat similar to those for single-carrier transmission (Fig. 7). However, the Q-penalties were relatively larger: 3.9 dB with a 5-ps skew, 3.5 dB with a 5-dB gain imbalance, 3.0 dB with a 10-degree phase error, and 2.7 dB with -10-dB crosstalk for the single carrier, as compared to 4.0, 3.9, 3.3, and 2.6 dB with the same respective impairments for dual-SC transmission. These results agree well with the phenomenon described previously, i.e., that IQ impairment mitigation techniques are particularly necessary for digital SC multiplexing systems.

Overall, the 16×4 WL MIMO equalizer outperformed the other equalizers, and the Q-penalty trends were almost the same as for single-carrier transmission (Fig. 7). Although excessive skew gradually degraded the 16×4 WL MIMO equalizer's performance, only 0.1-dB Q-penalties were observed up to 7 ps, and a Q-penalty of 0.5 dB appeared at 10 ps. For the other Tx impairments, the Q-factor differences were negligible between the 8×2 WL and 16×4 WL MIMO equalizers.

In contrast, the complex 16×4 MIMO equalizer showed relatively worse performance as compared with the complex 8×2 MIMO equalizer. It mitigated some of the Tx impairments, and the Q-penalty trends were similar to those for single-carrier transmission (Fig. 7); however, larger Q-penalties were observed when the Tx impairments reached large values. Specifically, the complex 8×2 MIMO equalizer in single-carrier transmission exhibited Q-penalties of 0.9 dB with a 5-ps skew, 2.6 dB with a 5-dB gain imbalance, 1.7 dB with a 10-degree phase error, and 1.8 dB with −10-dB crosstalk, as compared to 1.4, 3.2, 1.6, and 2.3 dB with the same respective impairments for dual-SC transmission with the complex 16×4 MIMO equalizer. The symbol rate in dual-SC transmission is half that in the single-carrier case, thus making it less tolerant of laser phase noise [14]. We assume that this phenomenon degraded the performance of the complex 16×4 MIMO equalizer, as it only includes the FO. Under the same conditions, the 16×4 WL MIMO equalizer showed almost the same Tx impairment performance as the 8×2 WL MIMO equalizer, which may indicate that the proposed 8×2 WL MIMO equalizer also has phase noise tolerance of more than 100 kHz.

Next, we evaluated the Rx impairment mitigation performance for 29-GBaud dual-SC PM-64QAM transmission.

In Fig. 10(a)–(d), the Q-factor is plotted as a function of the X-IQ skew, X-IQ imbalance, X phase error, and X-IQ crosstalk, respectively. For all cases, the 2×2 SL MIMO equalizer's performance deteriorated as the impairment increased, and the Q-penalties were slightly worse than in the single-carrier case. With both the 16×4 WL and complex 16×4 MIMO equalizers,

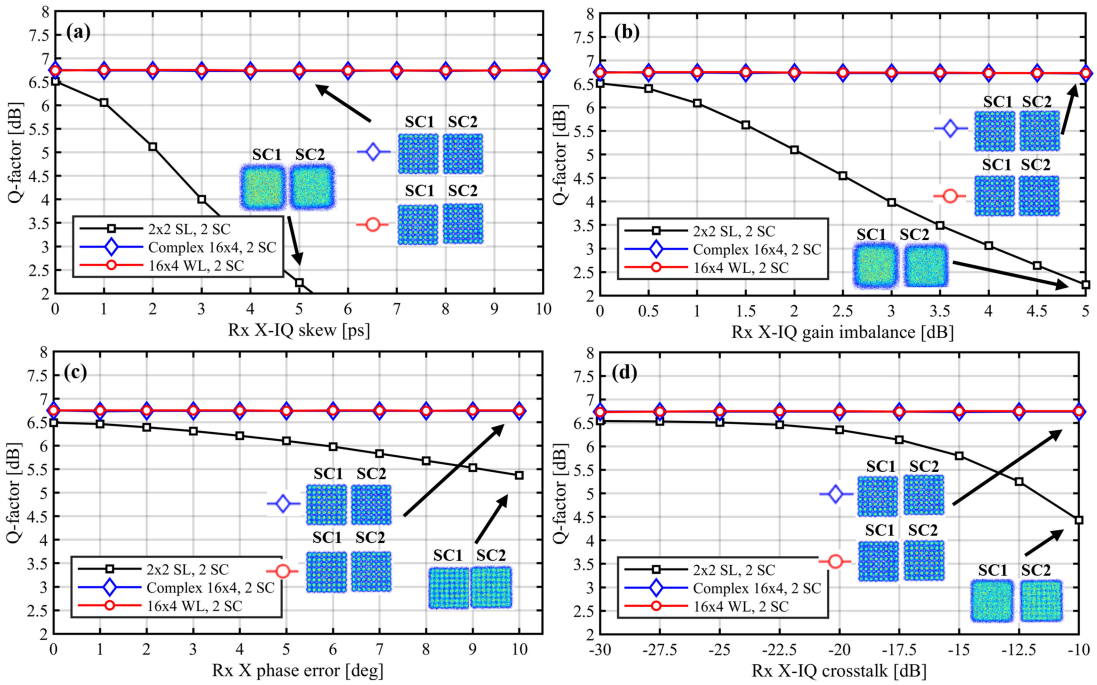

Fig. 10. Experimental results for 29-GBaud dual-SC PM-64QAM transmission with Rx impairments: (a) X-IQ skew, (b) X-IQ gain imbalance, (c) X phase error, and (d) X-IQ crosstalk.

no Q-penalties were observed up to a 10-ps skew, 5-dB gain imbalance, 10-degree phase error, and –10-dB crosstalk. These results show that the proposed WL MIMO equalizer effectively mitigated Rx impairments, and that it was unaffected by insufficient phase recovery even for dual-SC transmission.

Finally, we evaluated the proposed WL MIMO equalizer with multiple Tx and Rx impairments: a 5-ps Tx-IQ skew, 2.5-dB Tx-IQ imbalance, 4.3-degree quadrature phase error, -20-dB Tx-IQ crosstalk, 5-ps Rx-IQ skew, 2.5-dB Rx-IQ imbalance, 5-degree Rx phase error, and -20-dB Rx-IQ crosstalk. In this part of the experiment, we applied these impairments to both polarization signals. The impairments were selected as half the maximum values shown in Figs. 7–10. We assume that the proposed method can work with larger impairments, but the number of taps for a finite impulse response (FIR) filter may not be enough to compensate for such excess values. Fig. 11(a) shows constellations obtained for 58-GBaud PM-64QAM transmission with the 2×2 SL MIMO equalizer, the complex 8×2 MIMO equalizer, and the 8×2 WL MIMO equalizer. Clearly, the 2×2 SL MIMO equalizer suffered from strong transceiver impairment, as its Q-factors could not be measured. The complex 8×2 MIMO equalizer mitigated most of the impairments, with a Q-factor of 5.9 dB, but the proposed 8×2 WL MIMO equalizer improved the Q-factor to 6.4 dB. Fig. 11(b) shows the constellations obtained for 29-GBaud dual-SC PM-64QAM transmission with the 2×2 SL MIMO equalizer, the complex 16×4 MIMO equalizer, and the 16×4 WL MIMO equalizer. As in the single-carrier case, the 2×2 SL MIMO equalizer could not recover at all, while the complex 16×4 MIMO equalizer showed some impairment mitigation, with a Q-factor of 5.8 dB. In contrast, the proposed 16×4 WL MIMO equalizer improved

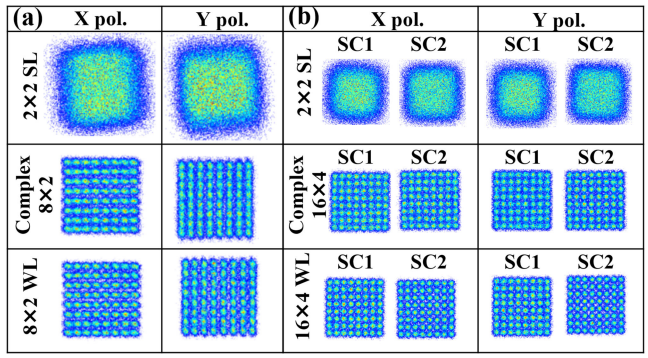

Fig. 11. Constellations obtained with multiple Tx and Rx impairments for (a) 58-GBaud PM-64QAM and (b) 29-GBaud dual-SC PM-64QAM transmission.

the Q-factor to 6.5 dB. The proposed method thus showed the capability to mitigate transceiver impairments even when different distortions occurred simultaneously.

Furthermore, it is noteworthy that we confirmed that no bit error after FEC was observed in the cases with the 8×2 WL and 16×4 WL MIMO equalizers, under all measurement conditions. By extracting certain measurement results for the normalized general mutual information (NGMI), an NGMI of 0.91 was obtained by the 8×2 WL and 16×4 WL MIMO equalizers with the multiple Tx and Rx impairments that were used for the results shown in Fig. 11.

Table I summarizes the experimental results in this work. The Q-penalty was defined via the Q-factor for each MIMO equalizer without any additional impairments.

TABLE I
SUMMARY OF THE EXPERIMENTAL RESULTS (CONV.: CONVENTIONAL)

Impairment			Q-penalty [dB]		
			2×2 SL	Conv.	Proposed.
Skew 10 ps	Tx	Single	> 5	> 5	0.1
		2 SC	> 5	> 5	0.5
	Rx	Single	> 5	< 0.1	< 0.1
		2 SC	> 5	< 0.1	< 0.1
Gain imb. 5 dB	Tx	Single	3.5	2.6	1.0
		2 SC	3.9	3.2	0.7
	Rx	Single	3.9	< 0.1	< 0.1
		2 SC	4.3	< 0.1	< 0.1
Phase err. 10 degree	Tx	Single	3.0	1.7	0.4
		2 SC	3.3	1.6	0.3
	Rx	Single	1.2	< 0.1	< 0.1
		2 SC	1.1	< 0.1	< 0.1
Crosstalk -10 dB at 29 GHz	Tx	Single	2.7	1.8	0.3
		2 SC	2.6	2.3	0.2
	Rx	Single	2.1	< 0.1	< 0.1
		2 SC	2.1	< 0.1	< 0.1
Multiple	Tx +Rx	Single	> 5	1.0	0.5
		2 SC	> 5	1.0	0.3

V. CONCLUSION

We proposed an 8×2 WL MIMO equalizer with independent complex filtering on IQ signals. Our method simultaneously compensates for polarization rotation, Tx impairments, Rx impairments, and carrier phase error by means of independent CDC. We analytically showed that the equalization provided by the proposed 8×2 WL MIMO equalizer is equivalent to the ideal signal demodulation process. Moreover, we extended the equalizer configuration for digital SC multiplexing, via a 16×4 WL MIMO equalizer for application to a pair of SCs to mitigate transceiver impairments.

Experimental results demonstrated that the proposed method could effectively mitigate various transceiver impairments in 58-GBaud PM-64QAM and 29-GBaud 2-SC PM-64QAM transmission. Our method and the conventional complex 8×2 MIMO equalizer showed similar Rx impairment compensation performance. However, our method outperformed the conventional method for Tx impairment mitigation. Specifically, in 58-GBaud PM-64QAM transmission over 100 km of SSMF, it achieved Q-penalties of 0.1 dB up to a 10-ps skew, 2.5-dB gain imbalance, 7.2-degree phase error, and –15-dB crosstalk. Moreover, the 29-GBaud 2-SC PM-64QAM transmission experiment showed similar Tx impairment mitigation performance, with Q-penalties of 0.1 dB up to a 7-ps skew, 2.0-dB gain imbalance, 7.2-degree phase error, and –15-dB crosstalk, even though the dual-SC approach is less tolerant of laser phase noise.

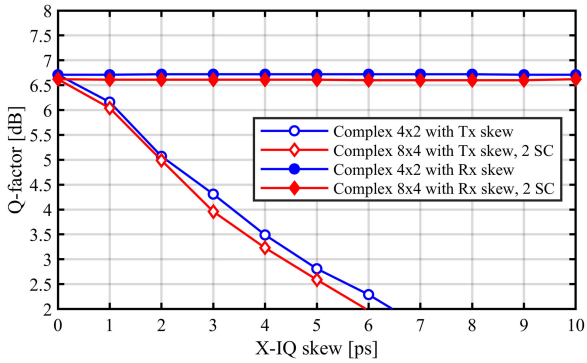

Fig. 12. Experimental results for 58-GBaud PM-64QAM / 29-GBaud dual-SC PM-64QAM transmission with X-IQ skew. The complex 4×2 MIMO equalizer was used for single carrier, and the complex 8×4 MIMO equalizer was used for dual SC.

APPENDIX I

In this study, we experimentally compared the linear transceiver impairment mitigation performance of the proposed 8×2 WL MIMO equalizer with the one of the conventional complex 8×2 MIMO equalizer. In order to clarify the advantages of our proposed method, we compare the results obtained with a simpler equalizer which may potentially be easier to implement. Therefore, we evaluate in this appendix the performance of a reported scheme based on a complex 4×2 MIMO equalizer with independent CDC [3], which is another option for adaptive linear impairment mitigation at the coherent receiver.

The complex 4×2 MIMO equalizer can be also applied for digital SC signal, modified to 8×4 MIMO configuration. We evaluated the linear impairment mitigation performance of the complex 4×2 MIMO equalizer for 58-GBaud PM-64QAM transmission, and that of the complex 8×4 MIMO equalizer for 29-GBaud dual-SC PM-64QAM transmission. In Fig. 12, the Q-factor is plotted as a function of the X-IQ skew in Tx or Rx. As the complex 4×2 MIMO equalizer works for Rx impairment compensation only, no Q-penalties were observed up to a 10-ps skew in Rx. However, as the complex 4×2 MIMO equalizer cannot mitigate IQ skew imbalance in Tx, the penalty was comparable to the 2×2 SL MIMO equalizer case of Fig. 7. The complex 8×4 MIMO equalizer showed almost same impairment mitigation performance with the complex 4×2 MIMO equalizer.

Therefore, if we consider the general case of a receiver demodulating the signal from a transmitter, which impairments are unknown, our 8x2 WL MIMO scheme offers better performance, although it may require more circuit resource for implementation.

APPENDIX II

In the proposed 8×2 WL MIMO equalizer with independent complex filtering on IQ signals, CDC is located before the 8×2 WL MIMO equalizer. From a practical perspective, it is difficult to estimate accumulated CD without any error, thus the residual CD needs to be compensated by the following MIMO equalizer. Therefore, we further evaluated the linear impairment mitigation performance of the proposed 8×2 MIMO equalizer

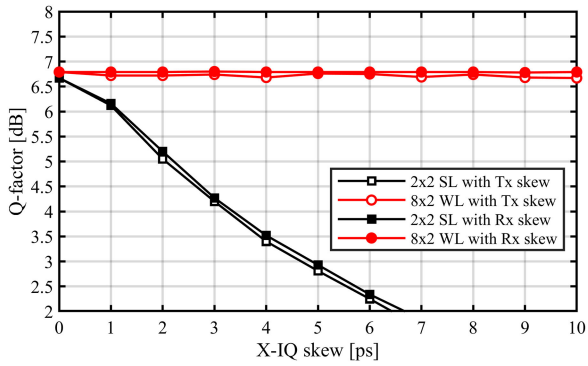

Fig. 13. Experimental results for 58-GBaud PM-64QAM transmission with X-IQ skew. The residual CD was set to +100-ps/nm.

for 58-GBaud PM-64QAM transmission with residual CD. The residual CD was set to +100-ps/nm by shifting the compensated CD values for the CDC part, as this value is clearly larger than the precision of our estimation. In addition, the 2×2 SL MIMO equalizer was used to measure the impact of linear impairments with residual CD. In Fig. 13, the measured Q-factor is plotted as a function of the X-IQ skew in Tx or Rx. For both equalizer cases, +100-ps/nm residual CD did not affect the performance, as Q-factors were almost same as in Figs. 7(a) and 8(a). Indeed, 21 taps for the 2×2 SL MIMO equalizer and for the proposed 8×2 WL MIMO equalizer were sufficient to compensate +100-ps/nm of CD and also an extra 10-ps of skew.

REFERENCES

[1] P. Winzer *et al.*, "Fiber-optic transmission and networking: The previous 20 and the next 20 years," *Opt. Exp.,* vol. 26, no. 18, pp. 24190–24239, Sep. 2018.

[2] A. Matsushita *et al.*, "High-spectral-efficiency 600-Gbps/carrier transmission using PDM-256QAM format," *J. Lightw. Technol.,* vol. 37, no. 2, pp. 470–476, Jan. 2019.

[3] R. Rios-Müller *et al.*, "Blind receiver skew compensation and estimation for long-haul non-dispersion managed systems using adaptive equalizer," *J. Lightw. Technol.,* vol. 33, no. 7, pp. 1315–1318, Apr. 2015.

[4] C. Fludger and T. Kupfer, "Transmitter impairment mitigation and monitoring for high baud-rate, high order modulation systems," in *Proc. Eur. Conf. Opt. Commun.*, Düsseldorf, Germany, 2016, pp. 1–3.

[5] M. Sato, M. Arikawa, H. Noguchi, J. Matsui, J. Abe, and E. L. T. De Gabory, "Mitigation of transmitter impairment with 4×2 WL MIMO equalizer embedding preliminary CPR," in *Proc. Opt. Fiber Commun. Conf Exhib.*, San Diego, CA, USA, 2022, pp. 1–3.

[6] J. Liang, Y. Fan, Z. Tao, X. Su, and H. Nakashima, "Transceiver imbalances compensation and monitoring by receiver DSP," *J. Lightw. Technol.,* vol. 39, no. 17, pp. 5397–5404, Sep. 2021.

[7] M. Arikawa *et al.*, "Adaptive equalization of transmitter and receiver IQ skew by multi-layer linear and widely linear filters with deep unfolding," *Opt. Exp.,* vol. 28, no. 16, pp. 23478–23494, Aug. 2020.

[8] T. Kobayashi *et al.*, "35-Tb/s C-band transmission over 800 km employing 1-Tb/s PS-64QAM signals enhanced by complex 8 × 2 MIMO equalizer," in *Proc. Opt. Fiber Commun. Conf.*, San Diego, CA, USA, 2019, pp. 1–3.

[9] M. Sandell *et al.*, "Novel IQ imbalance estimation for wideband MIMO OFDM systems with CFO," in *Proc. IEEE Glob. Commun. Conf.*, Waikoloa, HI, USA, 2019, pp. 1–6.

[10] E. P. da Silva and D. Zibar, "Widely linear blind adaptive equalization for transmitter IQ-imbalance/skew compensation in multicarrier systems," in *Proc. Eur. Conf. Opt. Commun.*, Dusseldorf, Germany, 2016, pp. 1–3.

[11] G. Bosco *et al.*, "Impact of the transmitter IQ-skew in multi-subcarrier coherent optical systems," in *Proc. Opt. Fiber Commun. Conf.*, Anaheim, CA, USA, 2016, pp. 1–3.

[12] O. Vassilieva, *et al.*, "Reach extension with 32- and 64 GBaud single carrier vs multi-carrier signals," in *Proc. Opt. Fiber Commun. Conf.*, Los Angeles, CA, USA, 2017, pp. 1–3.

[13] Q. Zhuge *et al.*, "Pilot-aided carrier phase recovery for M-QAM using superscalar parallelization based PLL," *Opt. Exp.*, vol. 20, no. 17, pp. 19599–19609, Aug. 2012.

[14] Xi Chen, *et al.*, "Experimental quantification of implementation penalties from laser phase noise for ultra-high-order QAM signals," in *Proc. Eur. Conf. Opt. Commun.*, Brussels, Belgium, 2020, pp. 1–4.

[15] Meng Qiu, *et al.*, "Laser phase noise effects and joint carrier phase recovery in coherent optical transmissions with digital subcarrier multiplexing," IEEE *Photon. J.,* vol. 9, no. 1, Feb. 2017, Art. no. 7901013.

[16] M. Mazur *et al.*, "Overhead-optimization of pilot-based digital signal processing for flexible high spectral efficiency transmission," *Opt. Exp.,* vol. 27, no. 17, pp. 24654–24669, Aug. 2019.